

# Research on Mechanical Properties of Stainless Steel/Copper Alloy Brazed Joints

Zong Hao

School of Materials and Chemistry, University of Shanghai for Science and Technology,  
Shanghai 200093, China

---

## Abstract

In order to study the electroplating of SnCu brazing material on stainless steel to braze copper alloy sheet, the effects of brazing material coating thickness, reflow temperature, reflow pressure and reflow time on the mechanical properties of the welded joints were investigated, respectively. Stainless steel is first plated with a primed Ni layer, then plated with Cu, and finally plated with SnCu brazing material, and then soldered with copper alloy sheet by reflow soldering, analyzed the organization and physical phase of the solder brazing material by SEM and EDS and XRD, and tested the strength of the soldered joints by micro-tensile machine. The experimental results show that the optimal process for welding is SnCu alloy plating brazing material thickness of 10 $\mu$ m, reflow soldering temperature of 270 $^{\circ}$ C, reflow pressure of 0.15MPa, reflow soldering time of 90s, at this case, the welded joints are completely generated Cu<sub>6</sub>Sn<sub>5</sub>, when the welded joints have the highest shear strength 27.5MPa.

## Keywords

SnCu Alloy Coating; Coating Welding; Joint Mechanical Properties.

---

## 1. Introduction

In electronic packaging and precision equipment, stainless steel and copper alloys need to be welded to achieve the effect of encapsulation. Due to the use of electronic packaging and precision equipment, it is necessary to use the welding method to connect the electronic components, welding methods such as pressure welding, fusion welding, brazing, etc., but the temperature of the pressure welding and fusion welding is too high, there is huge impact and damage on the properties of parent material<sup>[1-4]</sup>. In the low-temperature brazing methods, in order to control the thickness of the weld seam, it is necessary to use the coating welding method, and with the coating welding method, it is necessary to solve the problem that stainless steel and copper alloys are difficult to plating brazing, and the welded joints do not have high strength<sup>[5-7]</sup>.

Coating welding using the traditional method of stainless steel surface plating a layer of copper or nickel using high-temperature transient liquid phase diffusion connection (transient liquid phase bonding, TLP bonding), this method generating welded joints are also copper-tin compounds, tin-nickel compounds. In this case, the solder remelting point and mechanical properties have been improved; but this welding method and the welding time is too long, the welding temperature is too high, the welding efficiency is low, and the production operation is complicated<sup>[8-11]</sup>.

In this paper, the use of stainless steel plating a priming layer of Ni, and then plating a layer of Cu, and then plating SnCu alloy brazing material on top of the Cu, and then use the hot air heating table pressurized welding of copper alloy sheet. The use of hot air reflow soldering improves the joint welding efficiency and generates Cu-Sn compound joints in a short time, and the Cu-Sn compounds have high remelting temperatures (remelting temperature of Cu<sub>3</sub>Sn is 676 $^{\circ}$ C, remelting temperature

of  $\text{Cu}_6\text{Sn}_5$  is  $415^\circ\text{C}$ ), which can improve the service temperature of the welded joints and the strength of the welded joints<sup>[12-16]</sup>, and this paper focuses on the study of the effect of SnCu brazing thickness and welding process on the mechanical properties of welded joints (welding process mainly contains reflow temperature and reflow pressure, reflow time).

## 2. Experiment

### 2.1 Experimental Materials and Processes

Experimental samples selected 30mm, 30mm, 0.2mm 304 stainless steel sheet, this paper first use hydrochloric acid pickling to remove the oxide film on the surface of the stainless steel, and then pre-plating nickel plating copper, and finally plating SnCu brazing material coating. The samples were degreased before pickling.

Chemical degreasing was performed with 30 g/L NaOH, 25 g/L  $\text{Na}_2\text{CO}_3$ , and 30 g/L  $\text{Na}_3\text{PO}_4$  as degreasing solution at  $60^\circ\text{C}$  for 5 min.

Acid washing with 20% hydrochloric acid to remove the oxide film on the surface of titanium, pickling time is 3min.

Pre-nickel plating was performed with 130 g/L of  $\text{NiCl}_2 \cdot 6\text{H}_2\text{O}$  and 100 g/L of HCl as the pre-nickel plating solution, with nickel plate as the anode and stainless steel sheet as the cathode<sup>[17-18]</sup>. The current density was  $5\text{A}/\text{dm}^2$  at room temperature.

Copper plating was formulated with 200 g/L of  $\text{CuSO}_4 \cdot 5\text{H}_2\text{O}$  and 70 mL/L of  $\text{H}_2\text{SO}_4$ , with the addition of appropriate amount of brightener and plating solution stabilizer, current density  $2\text{A}/\text{dm}^2$ , room temperature, time 4 min, anode for phosphor bronze sheet, cathode for 304 sheet<sup>[19-20]</sup>.

The electroplating brazing material SnCu alloy solution was used  $\text{SnSO}_4:40$ ,  $\text{CuSO}_4:0.8$ ,  $\text{H}_2\text{SO}_4:100$ , citric acid:40, thiourea:0.08, sodium potassium tartrate 40, and hydroquinone:1.0 (g/L); the process conditions were as follows: plating density:  $1\text{A}/\text{dm}^2$ , plating solution temperature:  $30^\circ\text{C}$ , and plating time: 10 min. the cathode current efficiency was about: 70%. The prepared Cu-Sn alloy plating layer was gray-white, with bright, flat and dense surface, and the copper content in the plating layer was 0.5~2%<sup>[21-24]</sup>.

Coating welding using stainless steel plating good SnCu alloy plating brazing material, and the length of 10mm, 4mm wide copper alloy sheet, with hot air heating table for reflow soldering; in order to facilitate the calculation, the control of the welded area of  $4 * 4\text{mm}$ , the welded joints in the shape of a tower joint, through the universal tensile testing machine to measure the welded joints of the shear force, the welded joints of the shear strength calculation formula:

$$\sigma = F/S; \quad (1)$$

F-the maximum load force of the welded joint fracture.

S-the welded area of the welded joint, here is a fixed value of  $16\text{mm}^2$ .

$\sigma$ -the joint shear strength.

### 2.2 Performance and Characterization

1) Micro-tensile testing machine precisionline vario to measure the shear strength of welded joints, tensile speed 1mm/1min.

2) Using FALCON 500 Vickers hardness tester to measure the hardness of the welded joints, measurement along the Cu/(Cu-Sn) interface inclined  $15^\circ$  line, the measurement point and the Cu/(Cu-Sn) interface parallel spacing of about  $10 \mu\text{m}$ , load weights of about 0.05Kg, hold load time 10s.

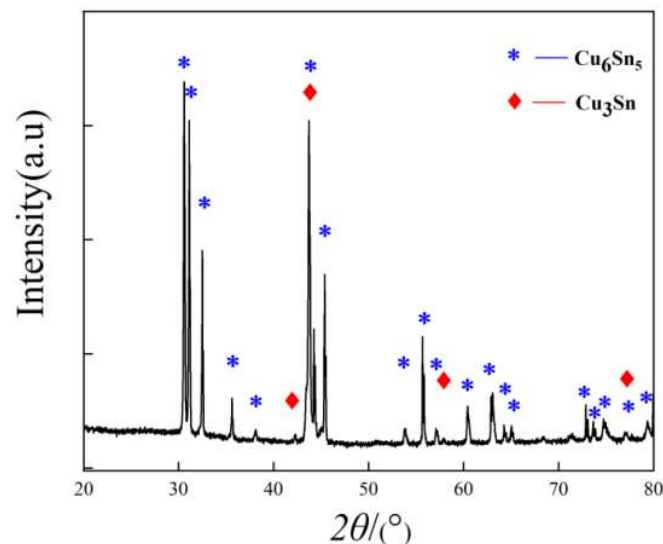
3) Scanning electron microscope(SEM) and X-ray spectrometer(EDS) (Fuhner Scientific Instruments Co., Ltd.) to analyze the weld morphology of the welded joints and welded joint fracture morphology.

4) X-ray diffractometer(XRD) model D8 ADVANCE was used to analyze the physical phase of the welded joints.

### 3. Experimental Results and Discussion

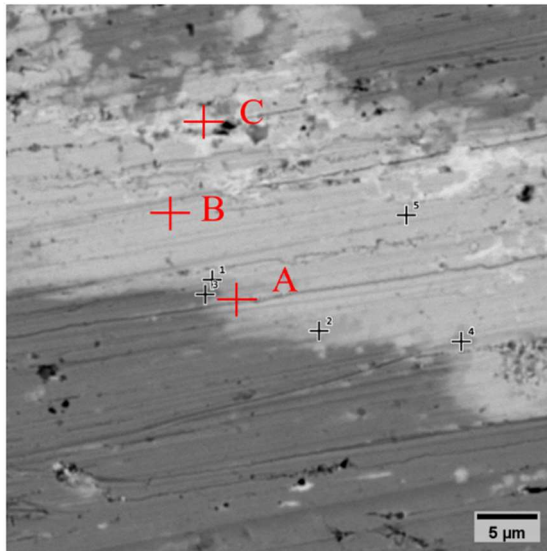
#### 3.1 The Organization and Microhardness Analysis of Welding Joint

Fig1. After the stainless steel and copper alloy sheet is completely welded, the XRD physical phase analysis of the weld brazing material is carried out, and after XRD analysis, it can be seen that its physical phase is mainly  $\text{Cu}_6\text{Sn}_5$ ,  $\text{Cu}_3\text{Sn}$ ; XRD analysis is shown below, comparing with the standard card, and the diffraction peaks on the top of the XRD are found to be corresponding to the  $\text{Cu}_6\text{Sn}_5$  and  $\text{Cu}_3\text{Sn}$  on the standard card, which confirms that the main component of the weld brazing material's physical phase is  $\text{Cu}_6\text{Sn}_5$ ,  $\text{Cu}_3\text{Sn}$ .

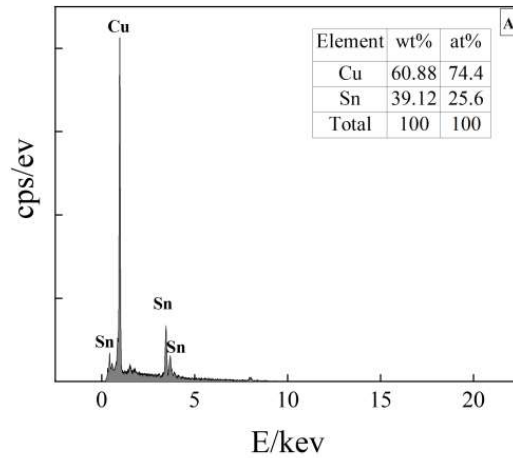


**Fig. 1** XRD analysis of physical phase of weld brazing material

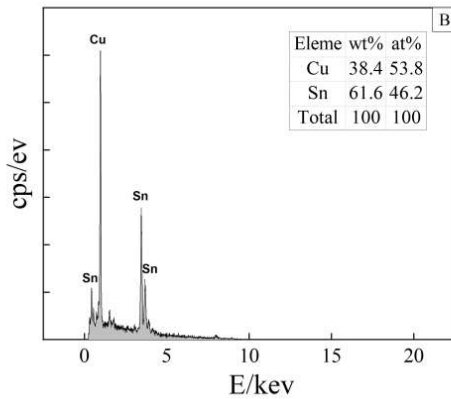
In order to further analyze the weld elements, Fig. 2 shows the enlarged SEM and EDS photos of the weld to analyze the different tissues of the weld. Since the composition of the plating solder is SnCu alloy solder, and the brazing material is plated Cu and copper alloy, respectively, the main elements of the solder composition in the weld seam are Cu and Sn. The main peaks shown on the top of the energy spectrum diagrams are the two elements of Cu and Sn, and the composition of the Cu-Sn compound is analyzed by the mass-to-atom ratio and the color characteristics of the weld seam area. The following figure shows the analysis results of different regions of the weld solder, from the SEM photo, point A hits in the dark gray region of the organization, EDS analysis of the A organization, from the analysis results, we can see that the mass ratio of the elements within the A is 60.88:39.12, which is converted into an atomic ratio of 74.4:25.8, the atomic ratio of close to 3:1, proving that the dark gray of organization is  $\text{Cu}_3\text{Sn}$ ; the point B in the figure hits in the light gray tissue, Within the EDS elemental analysis and results, it can be seen that the mass fraction ratio of Cu:Sn is 38.4:61.6, which translates into an atomic ratio of 53.8:46.2, and the atomic ratio is close to 6:5, so the light gray of organization is  $\text{Cu}_6\text{Sn}_5$ , and the white organization in the figure is pure Sn by EDS analysis; In summary, the copper-tin soldering organization of the dark grey organization is  $\text{Cu}_3\text{Sn}$ , the light grey is  $\text{Cu}_6\text{Sn}_5$ , the white organization is Sn, the white organization is Sn.



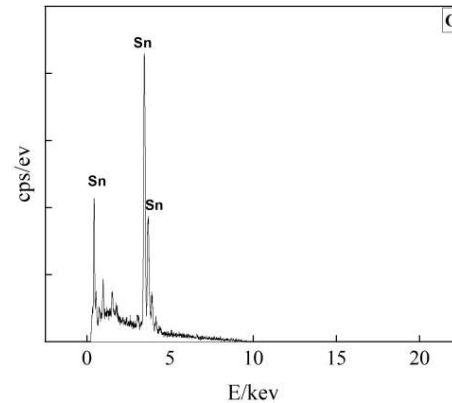
(a) SEM of the welded joint



(b) Dark grey organization



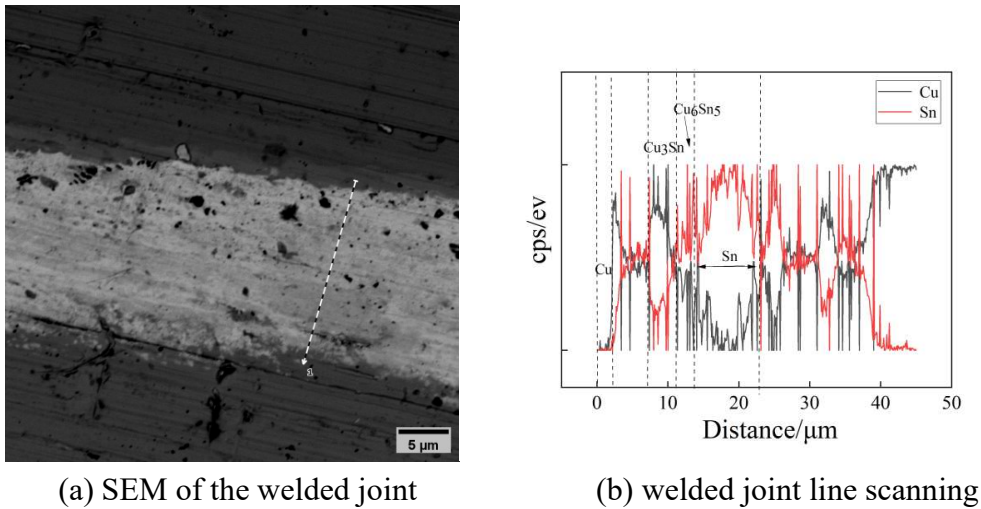
(c) Light grey organization



(d) White organization

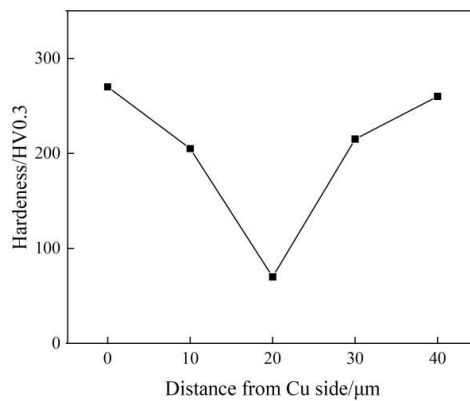
**Fig. 2** SEM photo and corresponding EDS photo of the welded seam

Fig. 3 is line scanning, in order to determine the different organizations formed in the Cu-Sn joints and the distribution of elements in the joints, along the Cu/(Cu-Sn) interface tilted 15° line, line scanning of the welded joints, From the fig. 3 found that the content of Cu and Sn with the distance, just starting from the top of the plated Cu, the line scanning elements of the highest content of Cu. As the distance increases, the Sn content increases, Cu<sub>3</sub>Sn is formed in 7-10μm, Cu<sub>6</sub>Sn<sub>5</sub> starts to appear as the distance increases, the farther away from the Cu plating the higher the content of Sn, in the middle of the 10-23μm, the content of Sn is the highest, and most of it exists in the form of Sn singlet; as the distance is close to the other side of the Cu alloy sheet, the content of Cu<sub>6</sub>Sn<sub>5</sub> starts to increase in the 25-30μm interval and the content of Cu<sub>6</sub>Sn<sub>5</sub> starts to increase close to the Cu alloy sheet. Cu<sub>3</sub>Sn appears in 30-35μm, and Cu<sub>6</sub>Sn<sub>5</sub> appears in a section in the middle of 35-38μm, so it can be seen that Cu<sub>6</sub>Sn<sub>5</sub> and Cu<sub>3</sub>Sn appear alternately. The last is on the copper alloy sheet, the energy spectrum is almost all Cu, from the line scanning can be seen Cu<sub>6</sub>Sn<sub>5</sub>, Cu<sub>3</sub>Sn, Sn content of alternating changes, from the following figure line scanning diagram can be seen in the welded joint, weld composition in the weld center is Sn, and close to the two sides of the Cu are Cu<sub>6</sub>Sn<sub>5</sub>, Cu<sub>3</sub>Sn.



**Fig. 3** SEM image and EDS line scan of welded joints

Fig. 4 for the microhardness of the weld solder, from the figure can be seen, the center of the weld about both sides of the hardness is the symmetrical shape, in the middle of the weld, and in the 20 $\mu$ m, the content of Sn is higher, so the microhardness is lower hardness average value of 70.5HV, because the content of Sn is the highest, so the microhardness of the weld is the lowest; close to the two sides of the Cu coating and copper alloy sheet when the content of Cu-Sn compounds is high, at this time the microhardness rises, which corresponds to the distribution of the Cu and Sn in the line scan of the fig. 3, the higher the Cu content, the higher the microhardness of the weld, the higher the content of Sn the lower the hardness of the weld. Therefore, the microhardness of the welding joint shows a symmetrical shape about the middle position.



**Fig. 4** Microhardness of welded seam

Fig. 5 shows the microhardness of the weld joint, from the above figure, it can be seen that figure (a) is the middle position area of the weld, and the main organization is Sn, while fig. 5 (b) is the area on both sides of the weld close to the Cu alloy and the coated copper, and the main organization is the Cu-Sn compounds, through the test of the microhardness, the following fig. 5(b) shows the microhardness of the Cu-Sn compounds, and the figure 5(a) is the microhardness of the Sn hardness; the average value of hardness of Sn in Fig.5 (a) is 67.5HV, while the average value of Cu-Sn compounds in Fig 5(b) is 278.3HV. By comparison, it can be seen that the hardness of Cu-Sn compounds is significantly higher than the hardness of Sn.

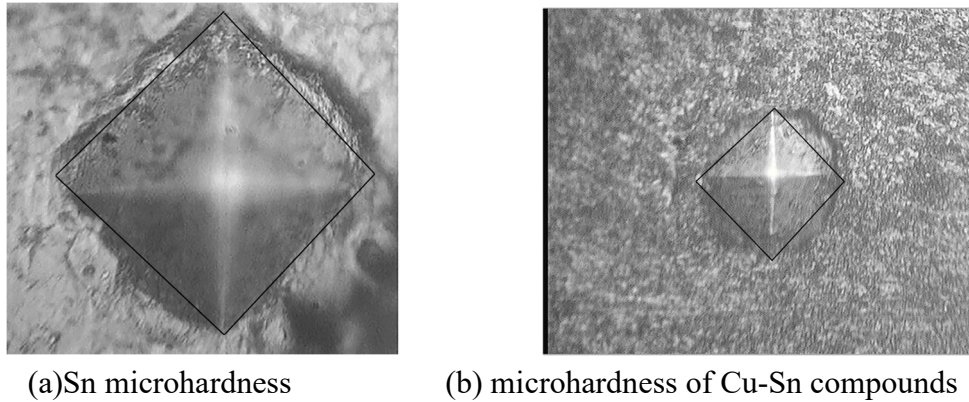


Fig. 5 Microhardness test

### 3.2 The Effect of Welding Process on the Strength of Welded Joints

The following fig. 6, in the reflow pressure 0.1MPa, reflow temperature 270°C, reflow time 90s. Study the effect of different SnCu brazing material coating thickness on the shear strength of welded joints. It can be seen from the figure with the increase of coating thickness, the shear strength of welded joints, first increased and then decreased and then unchanged, it can be seen from the figure, the coating thickness of 5 $\mu\text{m}$  to the plating thickness of 10 $\mu\text{m}$ , the strength of the welded joints grows very quickly, in the solder plating 5 $\mu\text{m}$ , welded joints are too poor strength, in the coating thickness of 10 $\mu\text{m}$ , strength of welded joints is the highest 27.5MPa; from 10 $\mu\text{m}$  to 30 $\mu\text{m}$ , the slope of the curve of shear strength is very small, and the strength of welded joints decreases very slowly, the strength of welded joints at 20 $\mu\text{m}$  and 30 $\mu\text{m}$  decreases slightly compared with the strength at 10 $\mu\text{m}$ , and the strength of welded joints is 25.4MPa and 24.3MPa, respectively, so that the shear strength of welded joints is maximum at the thickness of brazing material plating layer of 10 $\mu\text{m}$ .

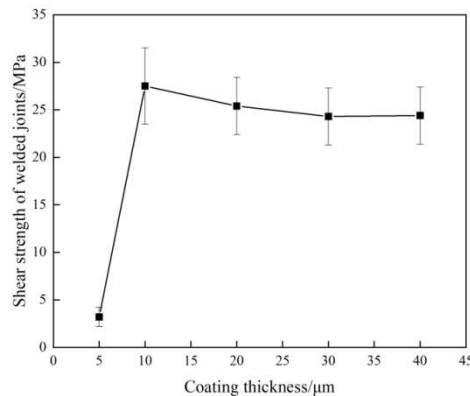
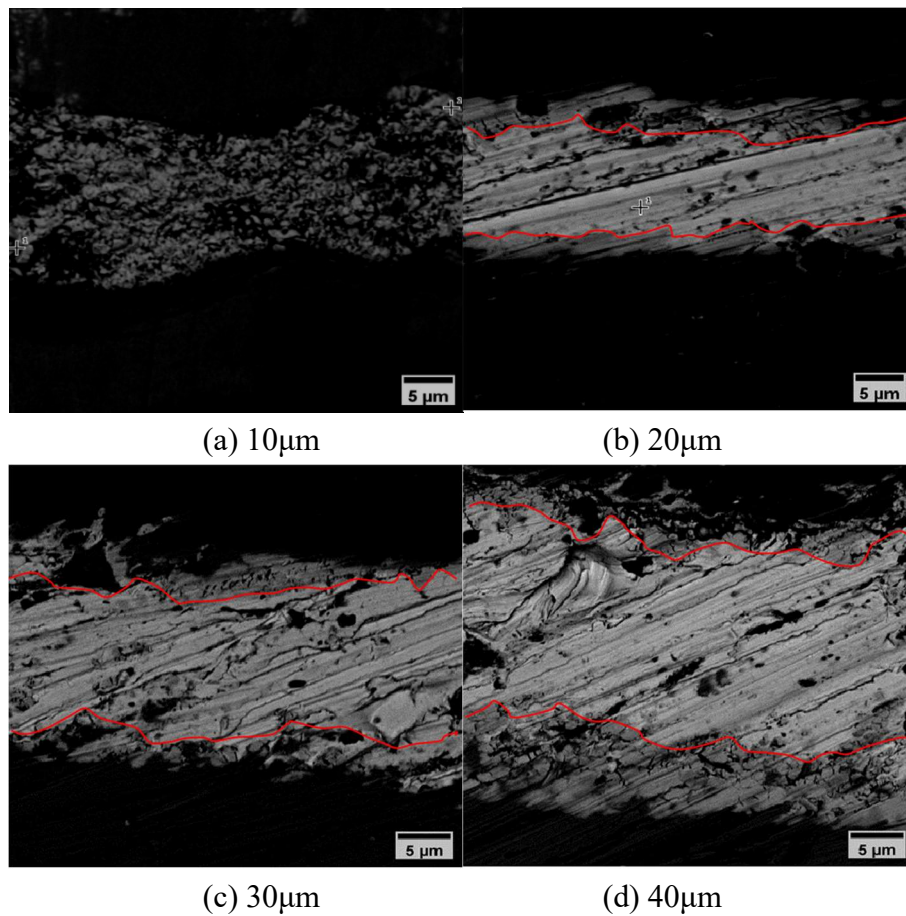


Fig. 6 Effect of SnCu alloy coating thickness on the shear strength of joints

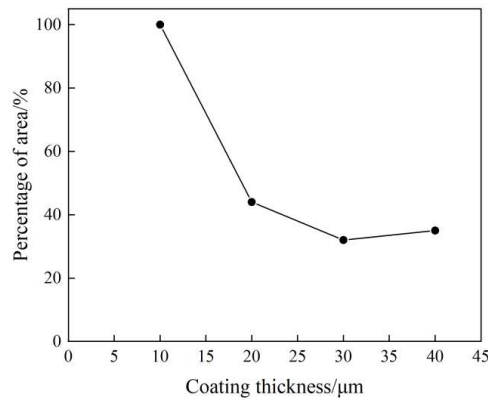
Analysis of the effect of brazing material thickness on the strength of welded joints, the reason why the shear strength of welded joints increases and then decreases with the thickness of the brazing material coating increasing; at the beginning of the brazing material coating is very thin for 5 $\mu\text{m}$ , and the Sn content of the brazing material is very small in the process of welding plus the air oxidation leads to the strength of welded joints is very poor, and it is difficult to form a welded joint structure, and there is no structure of 5 $\mu\text{m}$  of brazing material coating in the SEM photo of the fig. 7. Fig. 7(a) SnCu brazing material coating thickness of 10 $\mu\text{m}$ , the gray tissue in the figure is Cu-Sn compounds, from the above figure has proved that the white tissue is Sn, the light gray tissue is  $\text{Cu}_6\text{Sn}_5$ , the dark gray tissue is  $\text{Cu}_3\text{Sn}$ , the figure of the weld in the gray tissue is very high, the weld is completely generated by the Cu-Sn compounds; Fig. 7(b) brazing material coating thickness of 20 $\mu\text{m}$ , Cu-Sn

compound on both sides of the red line. with the increase of the thickness of the brazing material coating thickness of 20 $\mu\text{m}$ , brazing material coating thickness increases, the strength of the welded joint is weakened on the contrary, this is because of the increase in the thickness of the plating brazing material, under the same welding process, the thicker coating brazing material generated by the content of Cu-Sn compounds is less; Fig. 7(c) (d) brazing material coating thickness of 30 $\mu\text{m}$ , 40 $\mu\text{m}$ , the graph of the gray tissue in the figure is very little, the content of Cu-Sn compounds has been very small, and the vast majority of the area of the graph of the White Sn, the elevated content of Sn leads to a decrease in the strength of the welded joint, the thicker the solder coating layer, the lower the content of Cu-Sn compounds in the joint, the lower the strength of the welded joint.



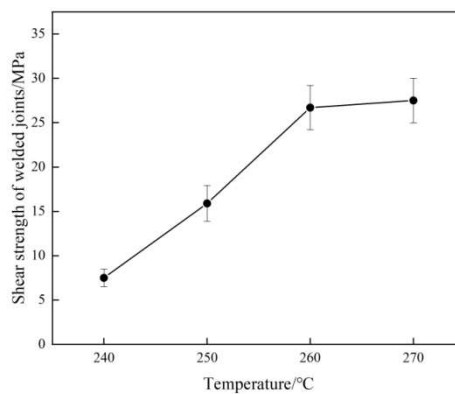
**Fig. 7** Weld morphology for different coating material thicknesses

Fig. 8, the relationship between the thickness of the brazing material coating and the percentage of area of Cu-Sn compounds, it can be seen from the figure, with the increase of the thickness of the brazing material coating, the percentage of area of Cu-Sn compounds in the weld layer decreases, in the case of the same welding process, the thinner SnCu brazing material coating, the greater the percentage of area of the Cu-Sn compounds generated; however, the brazing material thickness can not be too thin, the thickness of the brazing material coating of 5 $\mu\text{m}$ , brazing is very difficult to welding This is because the oxidation of the welding process, brazing material is too thin, the content of Sn is less, the welding process is easy to be completely oxidized, The brazing material coating 10 $\mu\text{m}$ , the coating is relatively thick and there is enough Sn to react with Cu, in a short period of time, in the middle of the weld layer interface compounds to generate Cu-Sn compounds, and the thicker coating, a short period of time reflow soldering is difficult to completely generate Cu-Sn compounds.



**Fig. 8** Area ratio of Cu-Sn compounds with different brazing coating thicknesses

Fig. 9 reflow temperature were changed, brazing material coating thickness of 10 $\mu\text{m}$ , reflow pressure of 0.15MPa, reflow time of 90s, the other process conditions remain unchanged to study the effect of reflow temperature on the shear strength of welded joints. From the figure, it can be seen that the strength of welded joints increases with the increase of welding temperature, and the highest strength of welded joints is 27.5MPa at 270 $^{\circ}\text{C}$ .



**Fig. 9** Effect of reflow temperature on the strength of welded joints

The effect of reflow temperature on the strength of welded joints, the strength of welded joints were increasing with welding temperature increasing. The higher temperature, the greater the solubility of Cu in Sn, the faster the enhancement of the reaction between Cu and Sn, the faster the growth rate of Cu-Sn compounds in the welded joints, and the rapid generation of Cu-Sn compounds in a short period of time. and the strength of Cu-Sn compounds itself is much higher than the strength of Sn, so with the increase in soldering temperature, the content of Cu-Sn compounds were increasing, the strength of the welded joints were increasing.

The fig. 10 shows the strength change of welded joints under different pressures when the thickness of weld brazing material plating is 10 $\mu\text{m}$ , welding temperature is 270 $^{\circ}\text{C}$ , and reflow time is 90s. It can be seen from the fig. 10 that the shear strength of welded joints increases first and then decreases, with the increase of welding pressure and the strength of welded joints is the best up to 27.5MPa.

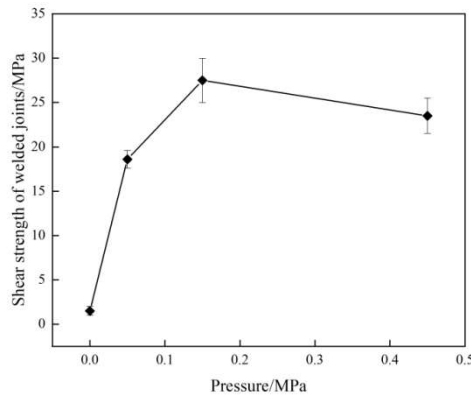


**Fig. 10** Effect of pressure on the strength of welded joints

The strength of welded joints first increased and then decreased with the increase in welding pressure. When the pressure is 0, SnCu brazing material and copper alloy gap is large, Cu and Sn reaction is weak, the welded joints generated by the lower content of Cu-Sn compounds, pressurization to reduce the gap between the SnCu brazing material and the copper alloy, to help the chemical reaction between the Cu and Sn, However, with the increase of welding pressure, the strength of the welded joint will be slightly weakened when the welding pressure is 0.45MPa, this is because the increasing pressure hindered the flow of Sn atoms of the plated brazing material, slowing down the reaction between Cu and Sn, and generating a reduction in the Cu-Sn compounds, and the strength of the welded joint was also reduced.

Fig. 11 shows that, with the increase of reflow time, the shear strength of the welded joint first increase and then decreases, the beginning of 30s, the strength of the welded joint is 15.8MPa, extend the reflow time, the strength of the welded joint grows very quickly, in the reflow time of 90s, the strength of the welded joint is the best 27.5MPa, but with the reflow time increases to 120s, the strength of the welded joint begins to weaken, and the strength of the welded joint decreases to 25.5MPa.

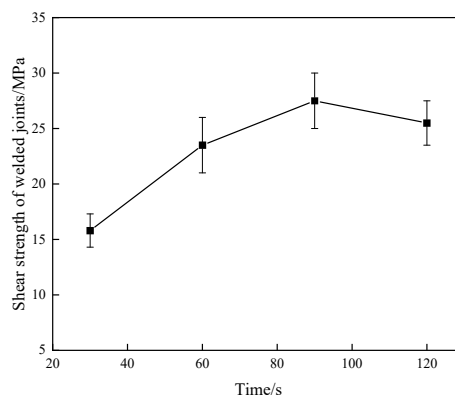


**Fig. 11** Effect of reflow time on the strength of welded joints

The strength of welded joints first increased and then decreased with the increase in reflow time, which is because as the welding time increases, the reaction time of Cu and Sn grows, and the content of Cu-Sn generated in the welded joints is increasingly high, Fig.12(a), the content of Cu-Sn

compounds generated in the reflow time of 30s is small; Fig. 12(b) the extension of the welding time at 60s, the content of Cu-Sn compounds in the welded joint is high. Fig. 12(c) at 90s of welding, the brazing material of the welded joint completely generates Cu-Sn compounds.12(d) at 120s of reflow time, the reflow time is too long, which leads to coarse particles of Cu-Sn compounds in the welded joints, which are in the form of particles of haphazard buildup, and results in the decrease of the strength of the welded joints. From the Hall-Petch formula, the larger the weld particles are, the poorer welded joint strength are. Therefore, with the prolongation of the reflow time, the strength of the welded joint increases first and then decreases.

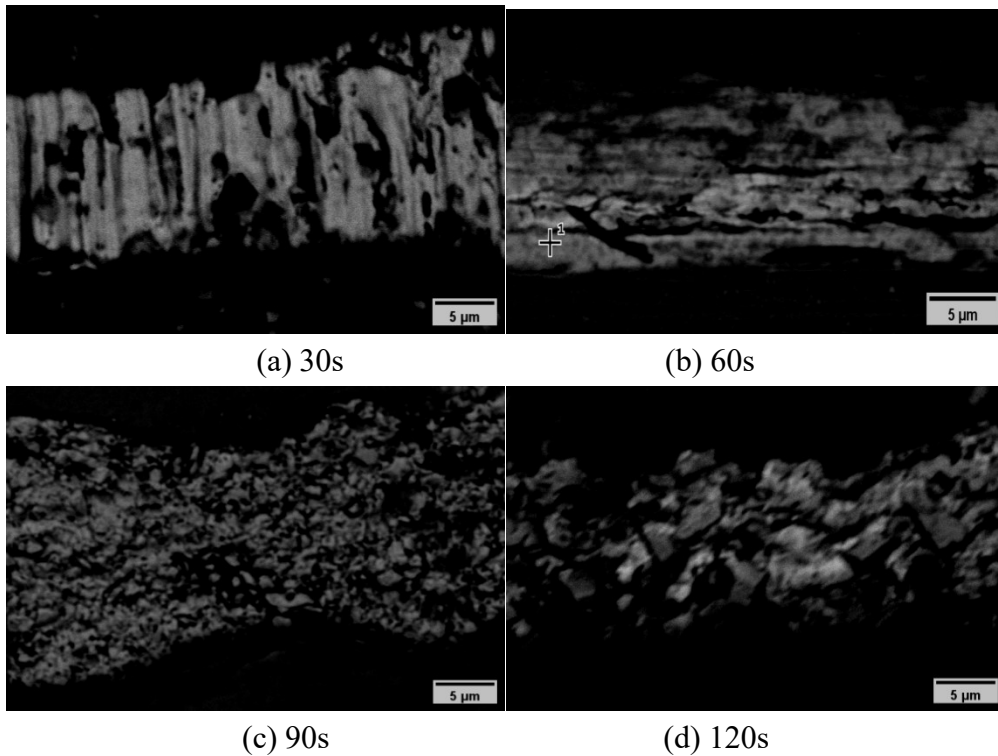


Fig. 12 Effect of reflow time on weld morphology

### 3.3 Welded Joint Fracture Analysis

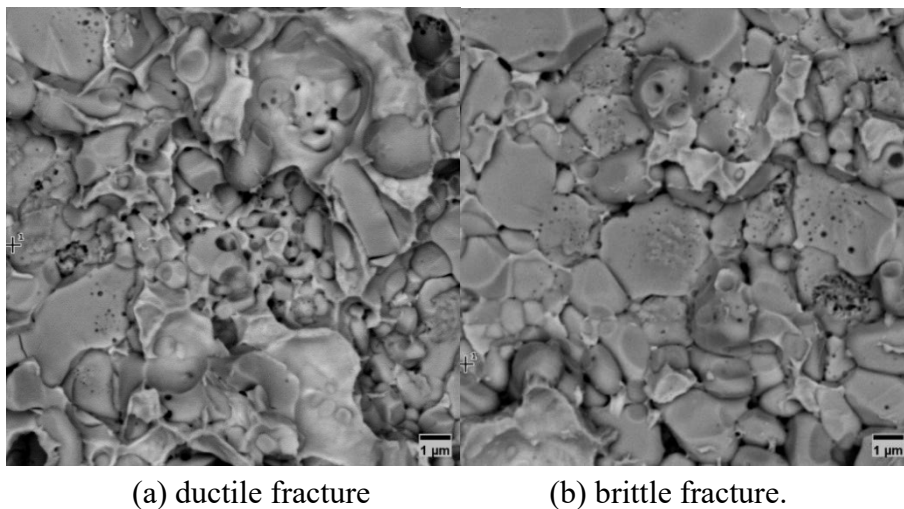


Fig. 13 Fracture morphology of welded joints

Fig. 13 in the SnCu brazing thickness of 10 $\mu$ m and the best welding process conditions, the morphology of the welded joint fracture; Fig.13 (a) and the small piece of stone-like for Cu<sub>6</sub>Sn<sub>5</sub>, its

fracture is obvious ductile nest-like, small stone-like Cu-Sn compounds pulling off the structure of the ductile nest left behind, at this time the fracture mode is the ductile fracture. Fig.13 (b) fracture interface of Cu-Sn compounds mainly for the large plate, large Cu-Sn compounds fracture interface like after scissors shear presented as a disintegration, disintegration structure of the main fracture mode is brittle fracture; therefore, Thus welded joints fracture by ductile fracture and brittle fracture.

#### 4. Conclusion

- (1). The hardness of Cu-Sn compounds is significantly higher than that of Sn; the microhardness of Sn is 67.5HV, while the hardness of Cu-Sn compounds is 278.3HV.
- (2). With the increase of the thickness of the solder coating layer, the welded joint strength increases first and then decreases, in the solder plating layer thickness of 10 $\mu$ m, the welded joint strength is the best 27.5MPa, as the thickness of the plating layer continues to increase, the content of Sn in the weld rises, the proportion of Cu-Sn compounds decreases, and the strength of the welded joints weakened.
- (3). The optimum process for coating welding is reflow temperature is 270°C, reflow pressure is 0.15MPa, and reflow temperature is 90s. The fracture mode of the joint fracture under the optimum welding process is ductile fracture and brittle fracture..

#### References

- [1] Liu H W, Huang L, Yu W Z, at al. Temperature Distribution Analysis of TIG Welding Process of Thin-Walled Stainless Steel and Red Copper[J]. Applied Mechanics and Materials, Trans Tech Publications Ltd, 2013, 423–426: 788–791.
- [2] Cui L H, Qiu R F, Shi H X, at al. Resistance Spot Welding between Copper Coated Steel and Aluminum Alloy[J]. Applied Mechanics and Materials, Trans Tech Publications Ltd, 2014, 675–677: 19–22.
- [3] Zhang M, Zhang Y, Li J, at al. Microstructure and Mechanical Properties of the Joint Fabricated Between Stainless Steel and Copper Using Gas Metal Arc Welding[J]. Transactions of the Indian Institute of Metals, 2021, 74(4): 969–978.
- [4] Pichuzhkin S A, Chernobaev S P, Vainerman A A. Mechanized Welding of Copper Alloys with Low-Alloy Structural Steels[J]. Chemical and Petroleum Engineering, 2016, 51(11): 861–864.
- [5] Choudhary R K, Laik A, Mishra P. Microstructure Evolution During Stainless Steel-Copper Vacuum Brazing with a Ag/Cu/Pd Filler Alloy: Effect of Nickel Plating[J]. Journal of Materials Engineering and Performance, 2017, 26(3): 1085–1100.
- [6] Kumar A, Ganesh P, Kaul R, at al. Study on requirement of nickel electroplating in OFE copper-316L stainless steel brazed joints[J]. The International Journal of Advanced Manufacturing Technology, 2016, 87(9): 2639–2651.
- [7] Kadhim A S, Aziz F L, Jasim A O. Investigate the interfacial reaction of copper/304 and copper/201 stainless steel joints[J]. AIP Conference Proceedings, 2023, 2830(1): 030032.
- [8] Brincker M, Kristensen P K, Söhl S, at al. Low temperature transient liquid phase bonded Cu-Sn-Mo and Cu-Sn-Ag-Mo interconnects – A novel approach for hybrid metal baseplates[J]. Microelectronics Reliability, 2018, 88–90: 774–778.
- [9] Chen W-Y, Duh J-G. Suppression of Cu<sub>3</sub>Sn layer and formation of multi-orientation IMCs during thermal aging in Cu/Sn–3.5Ag/Cu–15Zn transient liquid-phase bonding in novel 3D-IC Technologies[J]. Materials Letters, 2017, 186: 279–282.
- [10] Zhao H Y, Liu J H, Li Z L, at al. Non-interfacial growth of Cu<sub>3</sub>Sn in Cu/Sn/Cu joints during ultrasonic-assisted transient liquid phase soldering process[J]. Materials Letters, 2017, 186: 283–288.
- [11] Shao H, Wu A, Bao Y, at al. Microstructure evolution and mechanical properties of Cu/Sn/Ag TLP-bonded joint during thermal aging[J]. Materials Characterization, 2018, 144: 469–478.
- [12] Zhong Y, Zhao N, Ma H T, at al. Low Temperature Ni/Sn/Ni Transient Liquid Phase Bonding for High Temperature Packaging Applications by Imposing Temperature Gradient[A]. 2017 IEEE 67th Electronic Components and Technology Conference (ECTC)[C]. 2017: 411–416.

- [13] Ikeda H, Sekine S, Kimura R, et al. Heat Resistant Cu-Sn based Joint Paste for less than 30 $\mu$ m joint thickness[A]. 2019 International Conference on Electronics Packaging (ICEP)[C]. 2019: 74–78.
- [14] Chen S-W, Lee S-W, Yip M-C. Mechanical properties and intermetallic compound formation at the Sn/Ni and Sn-0.7wt.%Cu/Ni joints[J]. Journal of Electronic Materials, 2003, 32(11): 1284–1289.
- [15] Zhong W, Qin F, An T, et al. Mechanical properties of intermetallic compounds in solder joints[A]. 2010 11th International Conference on Electronic Packaging Technology & High Density Packaging[C]. 2010: 520–524.
- [16] Ohguchi K, Kurosawa K. An Evaluation Method for Tensile Characteristics of Cu/Sn IMCs Using Miniature Composite Solder Specimen[J]. Journal of Electronic Materials, 2016, 45(6): 3183–3191.
- [17] Xin T, Ajmera P K. Nickel electrodeposition studies for high-aspect-ratio microstructure fabrication for MEMS[A]. Smart Structures and Materials 2006: Smart Electronics, MEMS, BioMEMS, and Nanotechnology[C]. SPIE, 2006, 6172: 104–113.
- [18] Zhao Q, Geng S, Chen G, et al. Comparison of electroplating and sputtering Ni for Ni/NiFe<sub>2</sub> dual layer coating on ferritic stainless steel interconnect[J]. Corrosion Science, 2021, 192: 109837.
- [19] Lv Y, Geng S, Shi Z. Evaluation of electroplated copper coating on ferritic stainless steel for solid oxide fuel cells interconnects[J]. Journal of Alloys and Compounds, 2017, 726: 269–275.
- [20] Ning Z, He Y. Rapid electroplating of Cu coatings by mechanical attrition method[J]. Transactions of Nonferrous Metals Society of China, 2008, 18(5): 1100–1106.
- [21] Khaselev O, Zavarine I S, Vysotskaya A, et al. Electroplating and Properties of SnBi and SnCu for Lead-Free Finishes[J]. Transactions of the IMF, 2002, 80(6): 200–204.
- [22] Williams M E, Moon K-W, Boettinger W J, et al. Hillock and Whisker Growth on Sn and SnCu Electrodeposits on a Substrate Not Forming Interfacial Intermetallic Compounds[J]. Journal of Electronic Materials, 2007, 36(3): 214–219.
- [23] Nakadaira Y, Matsuura T, Tsuruya M, et al. Pb-free plating for peripheral/leadframe packages[A]. Proceedings Second International Symposium on Environmentally Conscious Design and Inverse Manufacturing[C]. 2001: 213–218.
- [24] Sarobol P, Pedigo A E, Su P, et al. Defect Morphology and Texture in Sn, Sn–Cu, and Sn–Cu–Pb Electroplated Films[J]. IEEE Transactions on Electronics Packaging Manufacturing, 2010, 33(3): 159–164.